



Published in final edited form as:

*Ultrasound Imaging*. 2012 January ; 34(1): 1–14.

## A three-dimensional, extended field of view ultrasound method for estimating large strain mechanical properties of the cervix during pregnancy

Michael House<sup>a</sup>, Helen Feltovich<sup>b,c,d</sup>, Timothy J Hall<sup>b</sup>, Trevor Stack<sup>e</sup>, Atur Patel<sup>e</sup>, and Simona Socrate<sup>f</sup>

<sup>a</sup>Department of Obstetrics and Gynecology, Tufts Medical Center, 800 Washington St, Boston MA 02111

<sup>b</sup>Department of Medical Physics, 1111 Highland Ave, University of Wisconsin, Madison WI 53703

<sup>c</sup>Department of Obstetrics and Gynecology, Intermountain Healthcare, 1034 N 500 W, Provo UT 84604

<sup>d</sup>Department of Obstetrics and Gynecology, 1 South Park, University of Wisconsin, Madison WI 53711

<sup>e</sup>Department of Biomedical Engineering, Tufts University, 4 Colby St, Medford MA 02155

<sup>f</sup>Harvard-MIT Division of Health Sciences & Technology, Massachusetts Institute of Technology, Cambridge MA 02139

### Abstract

Cervical shortening and cervical insufficiency contribute to a significant number of preterm births. However, the deformation mechanisms that control how the cervix changes its shape from long and closed to short and dilated are not clear. Investigation of the biomechanical problem is limited by 1) lack of thorough characterization of the three-dimensional anatomical changes associated with cervical deformation and 2) difficulty measuring cervical tissue properties *in vivo*. The objective of the present study was to explore the feasibility of using three-dimensional ultrasound and fundal pressure to obtain anatomically accurate numerical models of large-strain cervical deformation during pregnancy and enable non-invasive assessment of cervical tissue compliance. Healthy subjects (n=6) and one subject with acute cervical insufficiency in the midtrimester were studied. Extended field of view ultrasound images were obtained of the entire uterus and cervix. These images aided construction of anatomically accurate numerical models. Cervical loading was achieved with fundal pressure, which was quantified with a vaginal pressure catheter. In one subject, the anatomical response to fundal pressure was matched by a model-based simulation of the deformation response, thereby deriving the corresponding cervical mechanical properties and showing the feasibility of non-invasive assessment of compliance. The results of this pilot study demonstrate the feasibility of a biomechanical modeling framework for estimating cervical

---

**Corresponding Author:** Michael House, Department of Obstetrics and Gynecology, Tufts Medical Center # 360, 800 Washington Street, Boston, MA 02111, United States, Tel: 617 636 3200, Fax: 617 636 4202, mhouse@tuftsmedicalcenter.org.

Author disclosure statement: No competing financial interests exist.

mechanical properties *in vivo*. An improved understanding of cervical biomechanical function will clarify the pathophysiology of cervical shortening.

### Keywords

biomechanics; cervical insufficiency; finite element analysis; three-dimensional imaging; ultrasonography

---

## INTRODUCTION

Preterm birth affects close to 13% of pregnancies in the United States,<sup>1</sup> contributes \$26 billion to health care costs,<sup>2</sup> and accounts for more than 50% of neonatal deaths.<sup>3</sup> Survivors of preterm birth often experience severe consequences, such as cerebral palsy, respiratory morbidity, mental retardation, blindness, deafness, cardiovascular disease and cancer.<sup>4</sup> Two therapies are available, progesterone supplementation and cerclage (a stitch around the cervix), but these have not appreciably reduced the incidence of preterm birth.<sup>1,5-7</sup> This is likely because the approach to treatment, as well as research, has been simplistic while the pathways to preterm birth are complex.<sup>8,9</sup>

In a significant number of cases, preterm birth is associated with preterm deformation of the cervix. The clinical presentation of cervical deformation is cervical shortening.<sup>10-12</sup> The cervix is a cylindrical anatomical structure and forms the lower part of the uterus. In normal pregnancy, the cervix remains closed until term to permit fetal growth and development. Preterm birth is associated with early, undesired shortening, often in the absence of uterine contractility.<sup>10-12</sup> Since cervical shortening is a strong risk factor for preterm birth, serial evaluation of cervical length using transvaginal ultrasound is recommended to identify women at increased risk.<sup>13,14</sup>

Preterm cervical shortening could be caused, in part, by weakened mechanical properties of the cervical stroma. Cervical mechanical properties arise from its fibrous extracellular matrix,<sup>15</sup> which undergoes extensive remodeling during pregnancy to prepare for childbirth.<sup>16,17</sup> Cervical remodeling is apparent on physical examination as softening and shortening. In previous *in vitro* work, we developed a stringent protocol for measuring the large-strain mechanical properties of cervical tissue *in vitro*.<sup>18</sup> We showed that the large stress-strain response of the tissue was nonlinear and anisotropic and varied according to obstetric history.<sup>18,19</sup> Our *in vitro* work was extended by using numerical models from idealized anatomy and a computational framework to demonstrate cervical deformation associated with preterm birth.<sup>20,21</sup> However, this work was based on idealized conditions and did not relate to patient-specific data.

To establish a causal relationship between weakened mechanical properties and preterm cervical shortening, it is necessary to estimate tissue properties in individual patients. However, estimation of tissue properties *in vivo* presents significant technical hurdles. First, it is necessary to deform the cervix safely and reproducibly. Prior studies of *in vivo* tissue properties used biomechanical devices to deform the cervix<sup>22,23</sup> but biomechanical devices can be uncomfortable and inconvenient. Second, current biomechanical devices can only

access the external os but cervical ripening initiates at the internal os (the junction between the cervix and uterus), where the extracellular matrix composition and properties are different.<sup>24</sup> Last, cervical tissue exhibits a nonlinear large-strain response<sup>19</sup> but prior attempts to estimate tissue properties use a limited displacement range (1 – 3 mm).<sup>23,25</sup>

Fundal pressure is a safe and common clinical maneuver used to elicit cervical changes during pregnancy.<sup>11</sup> Fundal pressure is most often applied between 18 – 26 weeks gestational age. At this gestational age, the uterine fundus (top of the uterus) is palpable near the umbilicus. To elicit cervical changes, the clinician applies pressure to the uterine fundus with an examining hand while monitoring cervical length with transvaginal ultrasound. In most patients, the cervix does not change in response to fundal pressure. In some women, the cervix shortens in real time (the “dynamic” cervix). Dynamic shortening is a known risk factor for preterm birth.<sup>11</sup>

The goal of the present study was to explore the feasibility of using ultrasound and fundal pressure to obtain anatomically accurate numerical models of large-strain cervical deformation during pregnancy. To achieve this goal, extended field of view ultrasound images were used to obtain numerical models that encompassed the entire uterus and cervix. Fundal pressure was used for cervical loading and was quantified with a vaginal pressure catheter. We present preliminary data on estimation of cervical mechanical properties from one subject using this ultrasound-based method and a previously described inverse finite element framework developed for 3D ultrasound imaging.<sup>26</sup>

## METHODS

### Subject Selection

A cross-sectional study was performed at a single tertiary care center. The study was approved by the Institutional Review Board. Subjects were invited to participate either 1) at their second trimester fetal anatomy survey or 2) after admission to Labor and Delivery because of acute cervical insufficiency. Exclusion criteria included symptomatic uterine contractions, higher order multiple gestation, vaginal bleeding and known or suspected placenta previa. An informed consent was obtained before each scan. Patient demographics, pregnancy history and delivery details were obtained by review of medical records.

### Extended Field of View Ultrasound

The objective was to obtain an ultrasound image of the entire uterus and cervix appropriate for construction of numerical models (Fig. 1). To achieve this objective, it was necessary to register overlapping 3D volumes to obtain an adequate field of view. Image registration followed a three-step protocol (Fig. 1).

- 1) A series of six 3D ultrasound volumes were obtained using an iU22 Ultrasound System (Philips Medical Systems, Bothell, WA) with a 3D6-2 curved array transducer. The six volumes were saved on a DVD and transferred to a desktop computer for offline image processing.
- 2) The ultrasound volumes were converted into a multidimensional biomedical imaging format (AnalyzeImage 7.5, AnalyzeDirect, Overland Park, KS) using a previously

published protocol.<sup>27</sup> It was necessary to convert the ultrasound volumes to the Analyze format to allow for manual alignment and image fusion (see below)

3) The volumes were manually aligned and fused using a 3D voxel registration module (Analyze 7.0, AnalyzeDirect). The most useful image feature for registration was the border between the amniotic fluid and uterine wall. Sharp contrast was seen between the amniotic fluid and uterine wall. Hence, this feature could be used to align adjacent volumes. At the completion of the protocol, the six volumes had been converted into a single volume with an extended field of view covering the entire uterus and cervix (Figs. 1, 2).

### **Numerical Model from Extended Field of View Ultrasound**

A numerical model was obtained from the extended field of view ultrasound following a previously published protocol.<sup>27,28</sup> Briefly, 2D images were selected from the 3D volume and placed in the workspace of solid modeling software (Solidworks, Concord, MA). The anatomy of interest was traced on the 2D images and the tracings were combined into a solid model using software tools (Fig. 3). The solid models was exported in CAD format and imported into a commercial finite element program (ABAQUS, Providence, RI).

### **Vaginal Pressure Increase Associated with Fundal Pressure**

To quantify the increase in vaginal pressure associated with fundal pressure, an Urodynamic system (Dorado KT, Laborie, Ontario, Canada) was used. A vaginal pressure catheter (#CAT875, Laborie) was placed anterior to the cervix and vaginal pressure was read continuously (Fig. 4).

### **Cervical Displacement Associated with Fundal Pressure**

To measure cervical displacement associated with fundal pressure, it was necessary to use transperineal ultrasound (Fig. 4). The advantage of transperineal ultrasound was that the pelvic bone (symphysis pubis) was visualized in the same field of view as the cervix. The symphysis was used as a fixed reference to determine cervical displacement associated with fundal pressure.<sup>29</sup> Transperineal ultrasound did not interfere with vaginal pressure measurement.

### **Protocol**

The following protocol was used for each subject. First, the transabdominal scans were performed, which were used to obtain the extended field of view ultrasound image. Second, the vaginal pressure catheter was placed. Third, fundal pressure was applied for 5 seconds and cervical displacement was measured with transperineal ultrasound. Vaginal pressure was measured before and after fundal pressure with the pressure catheter. Fundal pressure was repeated a total of three times. The mean of the three measurements of vaginal pressure was recorded. The time required for subject involvement was 30 minutes.

## Magnetic Resonance Imaging

In 1 subject, MRI and ultrasound was performed on the same day to compare image features using these two modalities for corroboration. The MR scan was performed on a GE Signa HDxt 1.5T system with a single shot fast spin echo sequence (Fig. 1).

## Inverse Finite Element Analysis

We have previously described an inverse finite-element modeling framework for estimation of soft tissue mechanical properties using full-field deformation data obtained from 3D ultrasound.<sup>26</sup> Briefly, the pelvic anatomy was simplified, as shown in Figure 3, and streamlined so as to capture the biomechanics of cervical deformation while minimizing model complexity. The identified structures include (Table 2, Figs. 1, 3): the uterus and cervix; the fluid-filled amniotic sac (the fetus is not explicitly modeled); the endopelvic fascia and ligaments supporting the cervix; the “abdominal region” (an homogenized representation of the abdominal organs surrounding the uterus); the “abdominal fascia”, an outer layer representing abdominal fascia/muscle/skin; the pelvic floor; and the pelvic bones and spine (modeled as rigid supports/constraints).

The anatomy was modeled using both solid (continuum) and shell elements. The solid regions were modeled using continuum linear tetrahedron elements (3D, 4-node (C3D4), Abaqus) and the abdominal fascia, pelvic floor, and fetal membrane were modeled by general-purpose finite strain shell elements (S3, S4, Abaqus), with initial thicknesses of 1 cm for the fascia and pelvic floor and 1mm for the membrane. The separate regions of the model are endowed with suitable tissue properties. The amniotic sac was modeled as a fluid filled cavity with the volumetric compliance of water (i.e., a bulk modulus of 2.2 GPa), and the amniotic membranes were modeled as incompressible, hyperelastic with a polynomial strain energy function ( $C_{10}=2$  MPa,  $C_{30}=300$  kPa).

A simplified hyperelastic constitutive model was employed for the stroma of the cervix and the uterine walls. The constitutive model is a simplified implementation of the full constitutive model for cervical stroma.<sup>19,20</sup> The bulk response of the tissue, combining the volumetric contribution of the collagen network and the osmotic contributions of glycosaminoglycans and proteoglycans in the ground substance, is modeled as linear elastic with a bulk modulus of 10 MPa for both cervical and uterine stroma. The equilibrium shear properties of the stroma are primarily controlled by the collagen network. The collagen network is represented by an 8-chain model with Langevin statistics whose nonlinear response is prescribed by two material parameters: a small-strain (or “initial”) modulus  $\mu_0$ , which differs between the uterine and cervical stroma, and a locking stretch  $\lambda_L$ , fixed at  $\lambda_L=1.07$  for both cervical and uterine stroma, which controls the stiffening of tissue response (modulus increase) at large strains.<sup>20</sup> A gradual transition (3 mm) in material properties is established over a narrow section above the internal cervical os, to switch from the properties of the uterine walls, with  $\mu_0=10$  kPa, to the properties of the cervix. The initial modulus of cervical tissue, typically in a range  $\mu_{0-CRVX}=0.5-50$  kPa, is the primary fitting parameter to be determined through inverse FE modeling by matching the model predictions to the observed cervical deformation pattern. The abdominal fascia and pelvic floor were modeled as a linear isotropic elastic materials with Young’s moduli of 100 kPa and 1 MPa,

respectively, and Poisson's ratio  $\nu = 0.4$ . The endopelvic fascia and ligaments were modeled as elastic, transversely isotropic, with longitudinal and transverse Young's moduli of 100 kPa and 10 kPa, respectively, longitudinal shear moduli of 5 kPa, and isotropic volumetric response with a bulk modulus of 10 MPa. The abdominal region was modeled as linear elastic with a Young's modulus of 10 kPa. The bulk compliance of the abdominal region, defined in terms a homogenized Poisson's ratio (range  $\nu_{ABD} = 0.1-0.4$ ), is the secondary fitting parameter to be determined through inverse FE modeling by matching the model predictions to the measured vaginal pressure increase associated with fundal pressure.

Loading conditions on the model include gravity (in the posterior direction as the patient is supine during the exam) and an intrauterine pressure of 1 kPa. When the intrauterine pressure is applied to the model, the amniotic sac expands and comes in contact with the uterus; membrane adhesion to the uterus (rough contact with small sliding) is thereby assumed for the contact conditions between the membranes and the uterine inner surface. The application of fundal pressure is simulated by displacing the corresponding area (Figure 3) at the top boundary of the model 1.5 cm posterior and 3 cm inferior. The model was rigidly fixed along the posterior midline (spinal column) and around the pelvis inner surface.

The inverse modeling procedure to fit the primary ( $\mu_{0-CRVX}$ ) and secondary ( $\nu_{ABD}$ ) model parameters relied on an iterative approach with manual search to minimize error (mismatch) in the displacement of 6 fiducial markers (3 anterior and 3 posterior) placed along the sagittal midplane of cervix, at the internal os, midpoint, and external os. Bulk compliance of the abdominal organs (as measured by  $\nu_{ABD}$ ) was optimized to match the increase in pressure measured by the vaginal transducer when fundal pressure is applied.

## RESULTS

### Patient population

Table 1 shows the demographics of the study population. A total of 7 subjects were enrolled in the study. Six healthy subjects were recruited at the fetal anatomy survey. One subject with cervical insufficiency was recruited prior to the placement of a physical examination-indicated cerclage ("rescue" cerclage). This subject presented at 18 weeks with 2 cm of cervical dilation and fetal membranes prolapsed to the external os (Fig. 2). The subject with a cerclage entered spontaneous labor at 26 weeks gestation. The newborn weight was 1040 gm. The six healthy subjects delivered at term.

### Solid Model from Extended Field of View Ultrasound

Figure 1 shows a solid model superimposed on an extended field of view ultrasound image of the uterus and cervix. By inspection, the geometry of the uterus and cervix is adequately represented by the shape and volume of the solid model. The extended field of view ultrasound image was used to define the uterus and cervix but not the supporting anatomy such as the endopelvic fascia, and cardinal/uterosacral ligaments. Although the fascia and ligaments are biomechanically relevant, they are difficult to visualize with 3D ultrasound. However, our previous experience with MRI-based datasets<sup>20,28</sup> was a valuable aid to refine

the ultrasound-based model to include the endopelvic fascia, the cardinal and uterosacral ligaments and the pelvic floor.

Figure 2 shows a solid model corresponding to the subject with cervical insufficiency. The ultrasound image shows funneling of the amniotic membranes to the external os, which is captured by the solid model. Construction of the solid model from the ultrasound volumes is performed manually and it is a time-intensive task (approximately two days per subject).

### **Ultrasound – MRI correlation**

Figure 1 (right) demonstrates the correlation between the ultrasound image and the MRI image of the same patient. The boundary of the amniotic fluid and uterine wall was used as the anatomical landmark for image segmentation.

### **Numerical Model from Solid Model**

The computational domain was discretized (meshed) with tetrahedral elements as illustrated in Figure 3. Patient-specific computational models from four healthy subjects are shown. The time required to import each solid model into the FE framework and mesh the model was, approximately, 2 days per model. There was a significant improvement in efficiency gained with experience.

### **Vaginal Pressure and Anatomical Changes Associated with Fundal Pressure**

The mean  $\pm$  SD baseline vaginal pressure was  $1.64 \pm 0.27$  kPa (Fig. 4). This value was similar to previously reported values for vaginal pressure in non-pregnant patients undergoing routine clinical cystometry.<sup>30</sup> The mean (95% confidence interval) rise in vaginal pressure associated with fundal pressure was 0.62 (0.47 – 0.77) kPa. Fundal pressure was also associated with significant cervical displacement (Fig. 4).

### **Estimation of Cervical Mechanical Properties During Pregnancy**

Under the applied fundal pressure, the cervix descends in the pelvis and deforms against the supporting structures (fascia, ligaments, pelvic floor, abdominal organs), as illustrated in Fig. 4. The pattern of cervical deformation in relation to the surrounding organs provides and indirect measure of tissue compliance. A stiff cervix will tend to maintain its shape, while translating and rotating into the pelvis, transmitting higher loads to the surrounding organs which will deform to accommodate cervical displacement. In contrast, a soft cervix will not just translate and rotate but it will also change its shape and, in the most extreme conditions, funnel to accommodate the penetration of the amniotic sack in the cervical canal. The finite element model predictions of structural deformation will match the observed anatomical changes in cervical geometry due to fundal pressure only if the relative stiffness of the cervical tissue compared to the surrounding organs is properly captured. The measurement of vaginal pressure increase under fundal pressure provides an additional constraint against which the model must be calibrated, to ensure that the model can correctly estimate the magnitude of tissue properties rather than just their relative compliance. The iterative fitting procedure provided a value for the Poisson ratio of the abdominal region  $\nu_{ABD} = 0.2$  to yield a satisfactory match to the measured average rise in vaginal pressure of 0.6 kPa. Figure 5 illustrates the deformation-matching procedure. For the pilot example in



the figure, a suitable agreement between model predictions and measured tissue deformation was found for a cervical tissue modulus  $\mu_{0-CRVX}=6.7$  kPa. The position and attitude of the symphysis provides a reliable landmark against which the ultrasound images and the deformed finite element model can be registered.

## DISCUSSION

In this study, extended field of view ultrasound aided construction of anatomically accurate numerical models of the uterus and cervix. Fundal pressure was used for cervical loading, which was quantified with a vaginal pressure catheter. In one subject, the anatomical response to fundal pressure was matched by a model-based simulation of the deformation response, thereby providing an estimate of cervical mechanical properties. Results of this pilot study demonstrate the feasibility of the proposed biomechanical modeling framework to estimate cervical mechanical properties *in vivo*.

Obstetricians suspect weakened load bearing properties of the cervical stroma contribute to preterm birth. However, this hypothesis is difficult to prove. The lack of a method to measure cervical mechanical properties limits the opportunity for clinical investigation. Others have proposed biomechanical devices to estimate cervical mechanical properties in both pregnant<sup>22,23</sup> and non-pregnant women.<sup>31-34</sup> Also in development are quantitative ultrasound techniques to obtain objective information about cervical microstructure.<sup>35,36</sup> In addition, fundal pressure and transvaginal ultrasound has been used in a semi-quantitative manner to quantify the 2D cervical response to loading.<sup>37</sup> The present study is novel for 1) quantifying the response to fundal pressure with a pressure catheter and 2) using a 3D biomechanical modeling framework to estimate cervical mechanical properties during pregnancy.

Fundal pressure was associated with a significant rise in vaginal pressure. The rise in vaginal pressure was seen in all subjects, though some variability was seen. It is not surprising that variability was seen with this measurement. Fundal pressure was applied on the maternal abdomen. The pressure catheter was located in vaginal canal. Given distance between the pressure catheter and the applied load, a significant degree of variation in the measured rise of vaginal pressure was to be expected.

The most useful imaging feature for construction of anatomically accurate numerical models was the border between the amniotic fluid and uterine wall. Sharp contrast between sonolucent fluid and echogenic uterine wall allowed accurate reconstruction of uterine shape. The most challenging anatomical features were the cervix and surrounding endopelvic fascia. Endopelvic fascia is difficult to visualize with ultrasound. Prior experience with MRI datasets aided construction of the cardinal and uterosacral ligaments, which provided appropriate boundary conditions for the cervix in the biomechanical model.<sup>28</sup> Accurate numerical models of uterine and pelvic anatomy were essential to capture the large strain deformation response of the cervix during pregnancy.

The most significant limitation of the present study is the amount of time required to obtain anatomically accurate numerical models. No automatic segmentation tools were available



for the anatomy of interest. Thus, manual segmentation was performed and several days were required to convert ultrasound data to a numerical model. Semi-automated algorithms to speed segmentation of important structures will be an important improvement before this technique is applied in a clinical setting. Obstetrical imaging lends itself to automated segmentation because the boundaries between the amniotic fluid and uterine wall are readily identifiable. However, image segmentation has been applied less in ultrasound than CT or MRI because ultrasound image segmentation is strongly influenced by the quality of the data. Ultrasound data is complicated by multiple artifacts such as speckle, unclear boundaries, signal attenuation, shadows, and dropout.<sup>38</sup> Although there are challenges associated with ultrasound image segmentation, ultrasound is more practical than other imaging modalities. In addition, recent advances in spatial/temporal resolution and 3D volume imaging have improved data quality, and thus the renewed interest in ultrasound image segmentation. Improved resolution of the displacement field in the cervix following fundal pressure may also provide sufficient signal to capture the effects of inhomogeneous tissue properties, allowing the implementation of more refined simulation models with axial and radial gradients in cervical compliance.

Patient-specific inverse FE modeling techniques are a powerful tool but require an extensive and costly modeling effort, which is arguably beyond the scope of routine prenatal care. Rather, patient-specific models and inverse FE methods can be employed to develop a simplified assessment framework for clinical practice. The development of an alternative, simplified protocol to estimate a “cervical tissue compliance index” based solely on US-measured dynamic changes and pelvic deformation patterns under fundal pressure is an ambitious goal for the proposed methodologies, with direct clinical relevance.

The clinical consequence of weakened cervical load bearing properties is cervical shortening and cervical insufficiency. Although shortening clearly precedes preterm birth in many patients,<sup>11</sup> less clear is whether shortening is a cause of preterm birth or a consequence of a different pathophysiology. There is an important need in the field to clarify this question so that interventions to improve cervical function can be appropriately developed. The long-term goal of the present research is to provide a mechanistic basis for how the cervix stays closed in normal pregnancy but shortens in preterm birth.

In summary, we report a technique to use extended field of view ultrasound to obtain anatomically accurate numerical models of the uterus and cervix during pregnancy. The models were used with an inverse finite element framework to obtain preliminary estimates of cervical mechanical properties *in vivo*. Our proposed testing modality, which can safely assess the mechanical response of the cervical tissue at the internal os, could be extremely useful to both research and clinical applications. A better understanding of cervical biomechanical function will clarify the pathophysiology of normal and abnormal cervical shortening. An improved understanding of deformation mechanisms will point to therapies that aim to improve cervical performance and thus prevent spontaneous preterm birth

## ACKNOWLEDGEMENTS

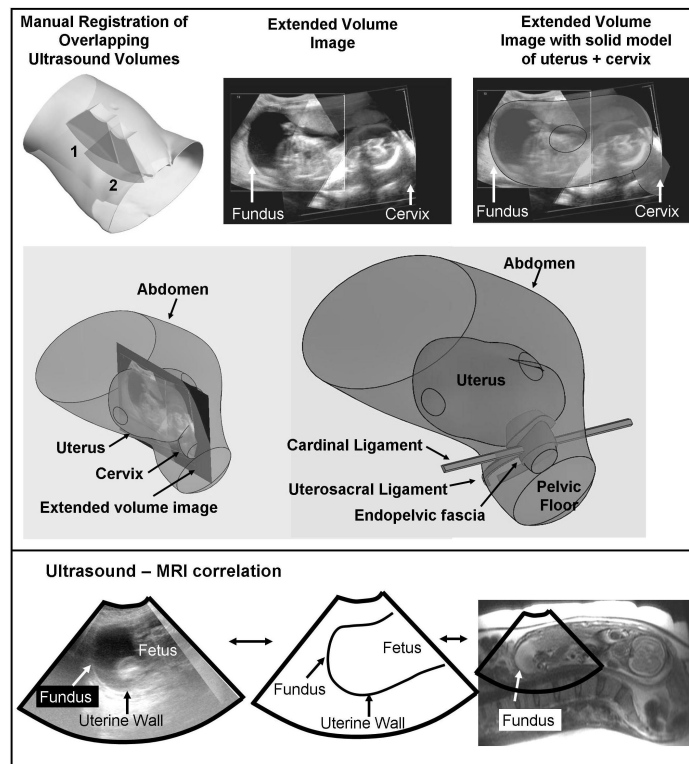
This work was supported by the Reproductive Scientist Development Program (NIH grant #2K12HD000849-21) and the March of Dimes Birth Defects Foundation. Additional funding from the Burroughs Wellcome Fund

Prematurity Initiative is gratefully acknowledged. Support from Dr. Tanaz Ferzandi and the Urogynecology department at Tufts Medical Center was appreciated.

## REFERENCES

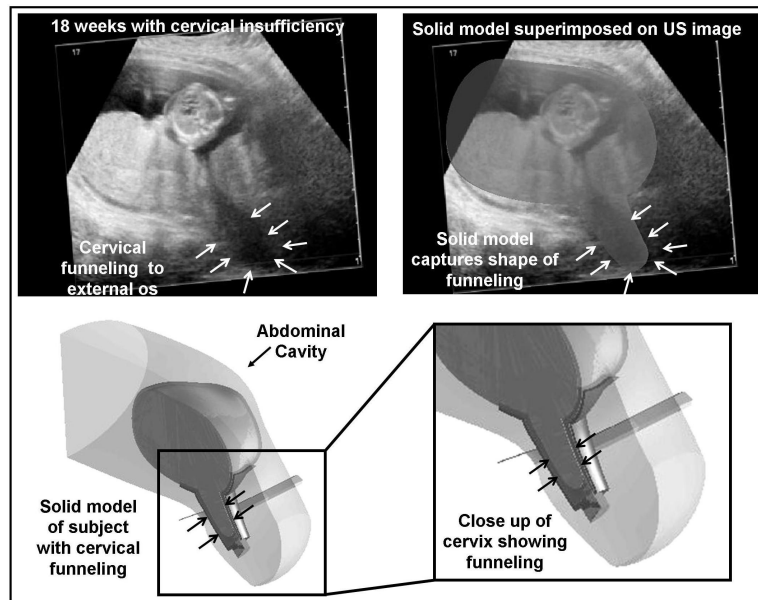
1. Martin JA, Hamilton BE, Sutton PD, et al. Births: final data for 2007. *Natl Vital Stat Rep.* 2010; 58:1–85. [PubMed: 21254725]
2. Institute of Medicine. *Preterm Birth: Causes, Consequences, and Prevention.* National Academies Press; Washington D.C.: 2006.
3. Mathews TJ, MacDorman MF. Infant mortality statistics from the 2006 period linked birth/infant death data set. *Natl Vital Stat Rep.* 2010; 58:1–31.
4. Spong CY. Prediction and prevention of recurrent spontaneous preterm birth. *Obstet Gynecol.* 2007; 110(2):405–415. [PubMed: 17666618]
5. Meis PJ, Klebanoff M, Thom E, et al. Prevention of recurrent preterm delivery by 17 alpha-hydroxyprogesterone caproate. *New England Journal of Medicine.* 2003; 348:2379–2385. [PubMed: 12802023]
6. Fonseca EB, Celik E, Parra M, Singh M, Nicolaides KH. Progesterone and the risk of preterm birth among women with a short cervix. *N Engl J Med.* 2007; 357:462–469. [PubMed: 17671254]
7. Owen J, Owen J, Hankins G, et al. Multicenter randomized trial of cerclage for preterm birth prevention in high-risk women with shortened mid-trimester cervical length. *Am J Obstet Gynecol.* 2009; 201:375, e371–378. [PubMed: 19788970]
8. Gravett MG, Rubens CE, Nunes TM, the GAPPS Review Group. Global report on preterm birth and stillbirth (2 of 7): discovery science. *BMC Pregnancy and Childbirth.* 2010; 10(Suppl 1):S2. [PubMed: 20233383]
9. Romero R. Vaginal progesterone to reduce the rate of preterm birth and neonatal morbidity: a solution at last. *Womens Health (LondEngl).* Sep; 2011 7(5):501–4.
10. Iams JD, Goldenberg RL, Meis PJ, et al. The length of the cervix and the risk of spontaneous premature delivery. *N Engl J Med.* 1996; 334:567–572. [PubMed: 8569824]
11. Owen J, Yost N, Berghella V, et al. Mid-trimester endovaginal sonography in women at high risk for spontaneous preterm birth. *JAMA.* 2001; 286:1340–1348. [PubMed: 11560539]
12. Heath VC, Southall TR, Souka AP, Elisseou A, Nicolaides KH. Cervical length at 23 weeks of gestation: prediction of spontaneous preterm delivery. *Ultrasound Obstet Gynecol.* 1998; 12:312–317. [PubMed: 9819868]
13. Ultrasonography in Pregnancy. ACOG Practice Bulletin No. 101. American College of Obstetricians and Gynecologists. *Obstet Gynecol.* 2009; 113:451–461. [PubMed: 19155920]
14. Iams JD, Berghella V. Care for women with prior preterm birth. *Am J Obstet Gynecol.* 2010; 203:89–100. [PubMed: 20417491]
15. House M, Kaplan DL, Socrate S. Relationships between mechanical properties and extracellular matrix constituents of the cervical stroma during pregnancy. *Semin Perinatol.* 2009; 33:300–307. [PubMed: 19796726]
16. Timmons B, Akins M, Mahendroo M. Cervical remodeling during pregnancy and parturition. *Trends Endocrinol Metab.* 2010; 21:353–361. [PubMed: 20172738]
17. Word RA, Li XH, Hnat M, Carrick K. Dynamics of cervical remodeling during pregnancy and parturition: mechanisms and current concepts. *Semin Reprod Med.* 2007; 25:69–79. [PubMed: 17205425]
18. Myers KM, Paskaleva AP, House M, Socrate S. Mechanical and biochemical properties of human cervical tissue. *Acta Biomater.* 2008; 4:104–116. [PubMed: 17904431]
19. Myers KM, Socrate S, Paskaleva AP, House M. A Study of the Anisotropy and Tension/Compression Behavior of Human Cervical Tissue. *J Biomech Eng.* 2010; 132:021003–021015. [PubMed: 20370240]
20. Paskaleva, AP. PhD Thesis Massachusetts Institute of Technology. 2007. Biomechanics of Cervical Function in Pregnancy - Case of Cervical Insufficiency. <http://dspace.mit.edu/handle/17211/42287>

21. House M, Socrate S. The cervix as a biomechanical structure. *Ultrasound Obstet Gynecol.* 2006; 28:745–749. [PubMed: 17063451]
22. Cabrol D. Cervical distensibility changes in pregnancy, term and preterm labor. *Semin Perinatol.* 1991; 15:133–139. [PubMed: 1876868]
23. Bauer M, Mazza E, Jabareen M, et al. Assessment of the in vivo biomechanical properties of the human uterine cervix in pregnancy using the aspiration test: a feasibility study. *Eur J Obstet Gynecol Reprod Biol.* 2009; 144(Suppl 1):S77–81. [PubMed: 19285777]
24. Word RA, Li X-H, Hnat M, Carrick K. Dynamics of cervical remodeling during pregnancy and parturition: mechanisms and current concepts. *Seminars Reprod Med.* 2007; 25(1):69–79.
25. Mazza E, Nava A, Bauer M, et al. Mechanical properties of the human uterine cervix: an in vivo study. *Med Image Anal.* 2006; 10:125–136. [PubMed: 16143559]
26. Jordan P, Socrate S, Zickler TE, Howe RD. Constitutive modeling of porcine liver in indentation using 3D ultrasound imaging. *J Mech Behav Biomed Mater.* 2009; 2:192–201. [PubMed: 19627823]
27. Lang CT, Iams JD, Tangchitnob E, Socrate S, House M. A method to visualize 3-dimensional anatomic changes in the cervix during pregnancy: a preliminary observational study. *J Ultrasound Med.* 2010; 29:255–260. [PubMed: 20103797]
28. House M, Bhadelia RA, Myers K, Socrate S. Magnetic resonance imaging of three-dimensional cervical anatomy in the second and third trimester. *Eur J Obstet Gynecol Reprod Biol.* 2009; 144:S65–69. [PubMed: 19297070]
29. Parikh R, Patel A, Stack T, Socrate S, House M. How the cervix shortens: an anatomical study using three dimensional transperineal ultrasound and image registration in singletons and twins. *J Ultrasound Med.* 2011 (in press).
30. Wall LL, Hewitt JK, Helms MJ. Are vaginal and rectal pressures equivalent approximations of one another for the purpose of performing subtracted cystometry? *Obstet Gynecol.* 1995; 85:488–493. [PubMed: 7898821]
31. van Duyl WA, van der Zon AT, Drogendijk AC. Stress relaxation of the human cervix: a new tool for diagnosis of cervical incompetence. *Clin Phys Physiol Meas.* 1984; 5:207–218. [PubMed: 6488727]
32. Zlatnik FJ, Burmeister LF. Interval evaluation of the cervix for predicting pregnancy outcome and diagnosing cervical incompetence. *J Reprod Med.* 1993; 38:365–369. [PubMed: 8320673]
33. Kiwi R, Neuman MR, Merkatz IR, Selim MA, Lysikiewicz A. Determination of the elastic properties of the cervix. *Obstet Gynecol.* 1988; 71:568–574. [PubMed: 3353048]
34. Anthony GS, Walker RG, Robins JB, Cameron AD, Calder AA. Management of cervical weakness based on the measurement of cervical resistance index. *Eur J Obstet Gynecol Reprod Biol.* 2007; 134:174–178. [PubMed: 17123693]
35. McFarlin BL, Bigelow TA, Laybed Y, et al. Ultrasonic attenuation estimation of the pregnant cervix: a preliminary report. *Ultrasound in Obstetrics & Gynecology.* 2010; 36:218–225. [PubMed: 20629011]
36. Feltovich H, Nam K, Hall TJ. Quantitative ultrasound assessment of cervical microstructure. *Ultrason Imaging.* 2010; 32:131–142. [PubMed: 20718243]
37. Pugatsch R, Elad D, Jaffa AJ, Eytan O. Analysis of cervical dynamics by ultrasound imaging. *Ann N Y Acad Sci.* 2007; 1101:203–214. [PubMed: 17303836]
38. Nobel JA, Boukerroui D. Ultrasound Image Segmentation: A Survey. *IEEE Trans Med Imaging.* 2006; 25:987–1010. [PubMed: 16894993]

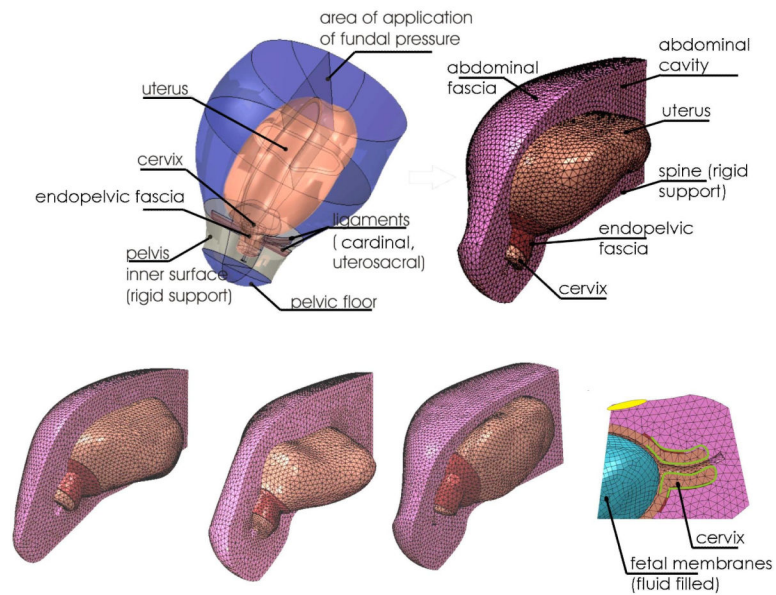


**Fig. 1.** Solid model superimposed on an extended field of view ultrasound image of the uterus and cervix

Six ultrasound volumes were manually registered to create a single, extended volume image of the entire uterus and cervix (top). Extended volume images were used to guide development of solid models that captured the shape of the uterus and cervix (middle). Note that only the cervix and uterus were seen with ultrasound images. The pelvic support anatomy (endopelvic fascia, cardinal ligament, uterosacral ligament) were not seen with ultrasound. Previous experience with pelvic MRI and knowledge of anatomic relationships were used to construct pelvic support anatomy. In one subject, MRI and ultrasound was performed on the same day showing correlation between the two imaging modalities (bottom)



**Fig. 2.**  
 Solid model corresponding to the subject with cervical insufficiency  
 A subject with cervical insufficiency was studied prior to the placement of a physical-examination indicated cerclage. The ultrasound images show protrusion of the amniotic sac to the level of the external os (white arrows, top). A solid model of this anatomy was constructed, which shows the marked cervical deformation associated with cervical insufficiency (bottom). The solid models accurately captured the anatomy of interest. Of note, this subject delivered at 26 weeks gestation.

**Fig.3.**

Numerical models of the uterus and cervix from 5 healthy subjects

The patient-specific solid models comprise the uterus and cervix as well as the surrounding abdominal/pelvic region and the cervical support structures. The model is imported into a finite element package (ABAQUS) and discretized (meshed) with tetrahedral elements. The four models shown come from healthy subjects who delivered at term. The model at the bottom right shows the fluid filled anatomic cavity. This cavity makes contact with the inner surface of the uterine wall.

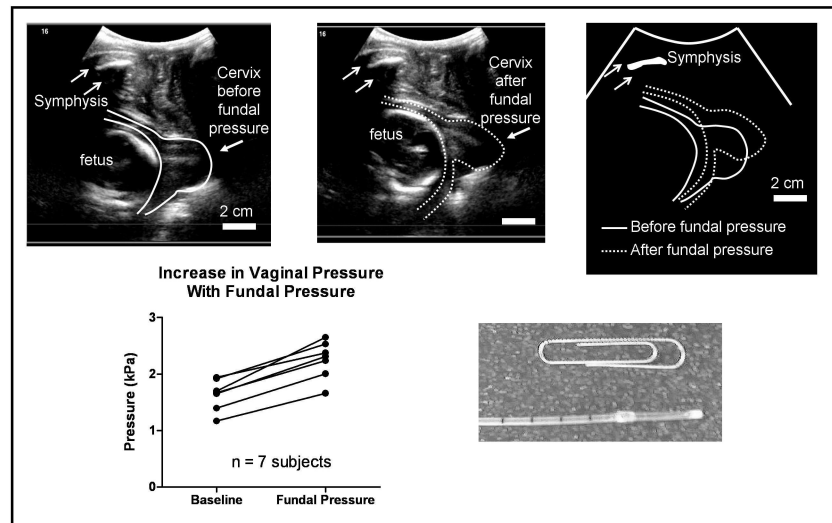


**Fig 4.** Quantification of cervical changes and vaginal pressure increases associated with fundal pressure. The ultrasound images show the cervical position before and after fundal pressure. Absolute change in cervical position was measured because a fixed bony landmark was present (symphysis, white arrows). The cartoon at right shows superposition of the cervical images before and after fundal pressure. This cervical displacement was used to guide modeling efforts (Fig. 5). The increase in vaginal pressure (bottom, left) was measured with a vaginal catheter (bottom, right) and was also used to guide modeling efforts. Each data point represents the mean of three measurements.



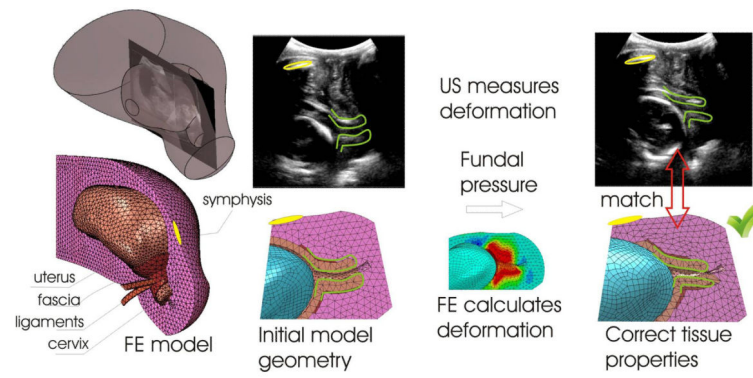


**Fig. 5.**

**Model-based estimation of cervical mechanical properties**

The mechanical properties of the cervix are systematically varied so that the model response matches the observed anatomical response. Only if correct tissue properties are used (right) will the model response match the anatomic response.

**Table 1**

## Subject demographics

Demographics	Healthy (n = 6)	Cerclage (n = 1)
Age (yr)	29 [27 - 33]	30
Body Mass Index (kg/m <sup>2</sup> )	33.3 ± 8.6	30.4
Ethnicity		
White, not Hispanic	5	1
Hispanic	1	
Primiparous (percent)	50 %	0 %
Gestational Age of Scan (weeks)	21 [19 – 24]	18
Gestational Age of Delivery (weeks)	40 [39 – 41]	26
Birthweight (gm)	3399 ± 666	1040

Data presented as mean ± standard deviation, median [range], or percent as indicated.

**Table 2**

Anatomic structures and model properties

Anatomy	Property	Comment
Uterus	Simplified version of full constitutive model <sup>19,20</sup> $\mu_0=10$ kPa	
Cervix	Simplified version of full constitutive model <sup>19,20</sup> $\mu_0= 0.5 - 50$ kPa	Final result for cervix tissue modulus = 6.7 kPa (see results)
Fetal membranes	Incompressible hyperelastic; Polynomial strain energy function ( $C_{10}= 2$ MPa, $C_{30}=300$ kPa); Thickness 1 mm	Contact with inner uterine surface (see methods)
Amniotic sac (fluid)	Bulk modulus 2.2 GPa; Intrauterine pressure 1 kPa	Volumetric compliance of water
Endopelvic fascia	Elastic, transversely isotropic; Longitudinal modulus 100 kPa; Transverse modulus 10 kPa Longitudinal shear modulus 5 kPa; Bulk modulus 10 MPa	Thickness 1 cm
Cardinal ligaments	See endopelvic fascia	
Uterosacral ligaments	See endopelvic fascia	
Abdominal cavity	Linear elastic; Modulus 10 kPa; Poisson's ratio 0.1 – 0.4	Final result abdominal Poisson's ratio= 0.2 (see results)
Abdominal fascia	Linear, isotropic elastic; Modulus 100 kPa; Poisson's ratio 0.4	
Pelvic floor	Linear, isotropic elastic; Modulus 1.0 MPa; Poisson's ratio 0.4; Thickness 1 cm	
Pelvic bones	Rigid constraint at pelvis inner surface	Figure 3
Spine	Rigid constraint at posterior midline	Figure 3